

17 β -ESTRADIOL POTENTIATES FIELD EXCITATORY POSTSYNAPTIC POTENTIALS WITHIN EACH SUBFIELD OF THE HIPPOCAMPUS WITH GREATEST POTENTIATION OF THE ASSOCIATIONAL/COMMISSURAL AFFERENTS OF CA3

M. T. KIM,^a W. SOUSSOU,^a G. GHOLMIEH,^c A. AHUJA,^b
A. TANGUAY,^{a,b,c} T. W. BERGER^{a,c}
AND R. D. BRINTON^{a,c,d*}

^aNeuroscience Program, University of Southern California, Los Angeles, CA 90089-2520, USA

^bDepartment of Electrical Engineering, University of Southern California, Los Angeles, CA 90089-0483, USA

^cDepartment of Biomedical Engineering, University of Southern California, Los Angeles, CA 90089-1451, USA

^dDepartment of Molecular Pharmacology and Toxicology, University of Southern California, School of Pharmacy, 1985 Zonal Avenue, Los Angeles, CA 90033-1033, USA

Abstract—We sought to determine the impact of 17 β -estradiol throughout the hippocampal trisynaptic pathway and to investigate the afferent fiber systems within CA1 and CA3 in detail. To achieve this objective, we utilized multielectrode arrays to simultaneously record the field excitatory postsynaptic potentials from the CA1, dentate gyrus, and CA3 of rat hippocampal slices in the presence or absence of 100 pM 17 β -estradiol. We confirmed our earlier findings in CA1, where 17 β -estradiol significantly increased field excitatory postsynaptic potentials amplitude (20% \pm 3%) and slope (22% \pm 7%). 17 β -Estradiol significantly potentiated the field excitatory postsynaptic potentials in dentate gyrus, amplitude (15% \pm 4%) and slope (17% \pm 5), and in CA3, amplitude (15% \pm 4%) and slope (19% \pm 5%). Using a high-density multielectrode array, we sought to determine the source of potentiation in CA1 and CA3 by determining the impact of 17 β -estradiol on the apical afferents and the basal afferents within CA1 and on the mossy fibers and the associational/commissural fibers within CA3. In CA1, 17 β -estradiol induced a modest increase in the amplitude (7% \pm 2%) and slope (9% \pm 3%) following apical stimulation with similar magnitude of increase following basal stimulation amplitude (10% \pm 2%) and slope (12% \pm 3%). In CA3, 17 β -estradiol augmented the mossy fiber amplitude (15% \pm 3%) and slope (18% \pm 6%) and the associational/commissural fiber amplitude (31% \pm 13%) and slope (40% \pm 15%). These results indicate that 17 β -estradiol potentiated synaptic transmission in each subfield of the hippocampal slice, with the greatest magnitude of potentiation at the associational/commissural fibers in CA3. 17 β -

Estradiol regulation of CA3 responses provides a novel site of 17 β -estradiol action that corresponds to the density of estrogen receptors within the hippocampus. The implications of 17 β -estradiol potentiation of the field potential in each of the hippocampal subfields and in particular CA3 associational/commissural fibers for memory function and clinical assessment are discussed. © 2006 IBRO. Published by Elsevier Ltd. All rights reserved.

Key words: estrogen, CA1, CA3, dentate gyrus, memory, hippocampus.

In a now classic series of electrophysiological field potential recording studies, Teyler, Foy and associates (Teyler et al., 1980; Chiaia et al., 1983; Foy and Teyler, 1983; Foy et al., 1984; Teyler and DiScenna, 1986) found that 17 β -estradiol (E₂) added to the bath increased excitability in the CA1 region of hippocampal slices from the male rat but not female, whereas testosterone had no effect on synaptic transmission on male slices but enhanced excitability in female rats in diestrus. The isomer, 17 α -estradiol, was without effect. Because the onset of the estrogen and testosterone effects was within minutes, Teyler and associates (Teyler et al., 1980) concluded that these responses were mediated by a membrane site of estrogen and androgen action that did not require transcriptional actions of estrogen and androgen receptors, respectively.

In vitro intracellular recordings from CA1 pyramidal neurons by Gu and Moss (1996) replicated and extended these findings to show that E₂ increased synaptic excitability by enhancing the magnitude of AMPA receptor-mediated responses but not NMDA responses most likely via a G-protein-coupled AMPA-dependent phosphorylation event. Because of the voltage-dependent blockade of the NMDA channel by Mg²⁺, and the slow kinetics of ligand-gated channel opening relative to that of the AMPA receptor subtype, there is only a minor NMDA receptor-mediated component of the excitatory postsynaptic potential (EPSP) evoked by low-frequency stimulation of glutamatergic afferents (Xie et al., 1997). The apparently exclusive estrogenic potentiation of non-NMDA receptor channels stood in contrast to a body of evidence demonstrating that estrogen-induced enhancement of neuronal morphology required activation of the glutamate NMDA receptor (Brinton et al., 1997a,b; Woolley et al., 1997). Because the Moss and Wong study was conducted using low frequency stimulation that is effective for activating the AMPA receptor but not the NMDA receptor (Xie et al., 1996), we sought to

*Correspondence to: R. D. Brinton, Department of Molecular Pharmacology and Toxicology, University of Southern California, School of Pharmacy, 1985 Zonal Avenue, Los Angeles, CA 90033-1033, USA. Tel: +1-323-442-1430; fax: +1-323-442-1489. E-mail address: rbrinton@usc.edu (R. D. Brinton).

Abbreviations: A/C, associational/commissural; CSD, current-source density; DCG-IV, 2-(2,3-dicarboxycyclopropyl) glycine; DG, dentate gyrus; EPSP, excitatory postsynaptic potential; ER α , estrogen receptor alpha; ER β , estrogen receptor beta; E₂, 17 β -estradiol; fEPSP, field excitatory postsynaptic potential; I/O, input/output; LTP, long-term potentiation; MEA, multielectrode array.

determine whether E_2 would potentiate NMDA receptor-mediated synaptic transmission under conditions favorable to NMDA receptor activation (Xie et al., 1992). Foy et al. (1999) using intracellular recording, under conditions of low Mg^{2+} and high-frequency stimulation investigated the acute effects of E_2 on pharmacologically isolated NMDA receptor-mediated EPSPs in CA1 pyramidal cells. Results of these analyses demonstrated that in the presence of E_2 , the AMPA receptor antagonist DNQX, and 0.1 mM Mg^{2+} , EPSPs evoked by Schaffer collateral stimulation were prolonged in duration, with slow rise and fall times characteristic of NMDA receptor-mediated synaptic responses (Foy et al., 1999). Identification of DNQX-resistant responses as being NMDA receptor mediated was confirmed by the effects by the NMDA antagonist, D-APV, which completely abolished residual evoked synaptic activity. In a corollary set of experiments, E_2 regulation of the AMPA receptor was investigated by pharmacologically inhibiting the NMDA receptor by D-APV. Under these conditions, E_2 potentiated the AMPA component in five of 14 cells (36%) which confirmed the previous findings of (Wong and Moss, 1991).

These studies were followed by analyses by Bi et al. (2000, 2001) who demonstrated that E_2 regulation of NMDA receptors required Src/ERK activation and that E_2 activation of the Src/ERK signaling pathway led to E_2 enhancement of long-term potentiation (LTP) and phosphorylation of the NR2 subunit of the NMDA receptor. Concurrent to these analyses, Woolley and coworkers (Rudick and Woolley, 2001; Rudick et al., 2003) found that estrogen attenuated GABA-mediated inhibition of CA1 pyramidal neurons and that the GABA release was increased by E_2 presynaptically.

While most electrophysiological analyses of E_2 action have focused on the CA1 region of the hippocampus, receptors for E_2 are present in each of the three-hippocampal subfields. Analyses to determine estrogen receptor distribution in hippocampus initially indicated the presence of estrogen receptors in the cell body of the pyramidal neurons, dentate gyrus (DG) granule cells, and interneurons (Loy et al., 1988; Weiland et al., 1997; Shughrue and Merchenthaler, 2000). Further electron microscopy and immunocytochemical analyses were conducted to determine precisely which estrogen receptor subtype was expressed in hippocampus. Results of these analyses indicate that estrogen receptor alpha ($ER\alpha$) is present in the cell body, dendritic spines, and axons of CA1, CA3 and DG (Shughrue et al., 1997; Weiland et al., 1997; Milner et al., 2001). $ER\alpha$ was detected in the nuclear compartment of the pre- and postsynaptic neurons, cytoplasmic/membrane compartment of hippocampal neurons, axons of pyramidal neurons, and within astrocytes (Woolley et al., 1997; Milner et al., 2001). However, the distribution of estrogen receptor beta ($ER\beta$) is not as uniform as its alpha counterpart. CA3 pyramidal neurons express the greatest abundance of nuclear and cytoplasmic $ER\beta$. Moreover, $ER\beta$ was detected in CA3 fibers in the stratum lucidum and in CA3 fibers that innervate the stratum radiatum of CA1 (Shughrue et al., 1997; Mitra et al., 2003; Nishio et al.,

2004). Results of our recent analyses indicate that activation of both $ER\alpha$ and $ER\beta$ can promote estrogen-associated function in hippocampal neurons (Zhao et al., 2004). Moreover, E_2 induced a rise in intracellular calcium within the soma and processes, consistent with the compartmental localization of ER (Zhao et al., 2005).

To address the broad question of whether estrogen potentiates synaptic transmission within each subfield of the hippocampus, we used multielectrode arrays (MEA) that enable simultaneous *in vitro* recording of activity from multiple sites within the hippocampal subfields (DG, CA3 and CA1). To selectively activate specific hippocampal afferents and to record from their respective targets high-density arrays were designed and fabricated. The high-density arrays also permitted acquisition of current sink and sources with electrodes recording from activated dendritic zones generating the extracellular current sink (negativity) as a consequence of positive ion influx whereas electrodes in adjacent regions recorded the extracellular current source (positivity) (Urban and Barrionuevo, 1996; Yeckel and Berger, 1998).

The current study addressed two issues: 1) whether E_2 potentiation of synaptic transmission in the hippocampus is limited to the CA1 region or whether it occurs throughout the trisynaptic pathway of the hippocampus and 2) which afferents in CA1 and CA3 when stimulated contribute to E_2 -induced potentiation. Results of these analyses indicate that E_2 potentiation of synaptic transmission is not unique to CA1 but is inducible in each subfield of the trisynaptic hippocampal system. Moreover, E_2 potentiation of synaptic transmission was greatest in CA3 at the associational/commissural (A/C) fibers that innervate the pyramidal neurons in the CA regions ipsilaterally and contralaterally.

EXPERIMENTAL PROCEDURES

Animals

Use of animals was approved by the Institutional Animal Care and Use Committee at the University of Southern California (Los Angeles, CA, USA; protocol no. 10256). All experiments conformed to the Animal Welfare Act, Guide to Use and Care of Laboratory Animals, and the US Government Principles of the Utilization and Care of Vertebrate Animals Used in Testing, Research and Training guidelines on the ethical use of animals. In addition, the minimal number of animals required for these experiments was used, and their suffering was minimized. Adult male Sprague–Dawley rats were purchased from Harlan Sprague Dawley (Indianapolis, IN, USA). They were housed under controlled conditions of temperature (18–24 °C), humidity (30–70%) and light (12-h light/dark), and received food and water *ad libitum*.

Acute slice preparation

Adult male white Sprague–Dawley rats were anesthetized with halothane prior to decapitation. The hippocampi were dissected out from the rat brains and directly immersed in an ice-cold ACSF (NaCl, 128 mM; KCl, 2.5 mM; NaH_2PO_4 , 1.25 mM; $NaHCO_3$, 26 mM; glucose, 10 mM; $MgSO_4$, 2 mM; ascorbic acid, 2 mM; $CaCl_2$, 2 mM, aerated with a mixture of 95% O_2 and 5% CO_2). Slices 400 μm thick were cut transversely with respect to the longitudinal axis of the hippocampus using a VT1000S vibratome (Leica, Wetzlar, Germany). The slices were then bathed in ACSF at 32 °C for at least one hour.

Extracellular recordings

The MEA system (www.multichannelsystems.com, Egert et al., 1998) is a commercially available recording system for MEAs. The MEA used in experiments on the entire hippocampal slice had a planar 8×8 grid configuration with 200 μm inter-electrode distance and an electrode diameter of 30 μm . The electrode conductors were gold based with tips covered with titanium nitride. The insulation layer consisted of silicon nitride. The high-density MEAs were developed to stimulate and record from select anatomical fiber systems within CA1 and CA3. The MEA has a planar 3×20 formation with 50 μm inter-electrode distance and an electrode diameter of 28 μm (Gholmieh et al., 2005). The electrode conductors are indium tin oxide based covered with chromium/gold. The insulating layer consisted of silicon nitride. The entire MEA system consists of an array, pre-amps, a data acquisition board and software. Data were sampled at 25 kHz per channel and processed using MCS software (MCRack v 2.2.2).

Experimental protocol

A 400 μm thick hippocampal slice was positioned over the MEA with the assistance of an inverted microscope (DMIRB, Leica). The submerged slice was held secure in place with a nylon mesh. The relative position of the slice with respect to the array was documented with a digital camera (Spot Model 2.0.0). The slice was perfused with ACSF (as listed above but with the Mg^{2+} concentration decreased to 1 mM) at a fixed flow rate (2–3 ml/min), and was heated to 32–33 °C. For the first set of experiments, a pair of electrodes in the MEA was used to deliver bipolar biphasic current stimulation to the DG afferents (perforant path, preferably the medial one), CA3 afferents (A/C fibers and mossy fibers), and the CA1 afferents (Schaffer collaterals), sequentially. For the second set of experiments, a pair of electrodes in the high-density MEA was used to deliver bipolar biphasic current stimulation to the apical afferents in CA1 (Schaffer collaterals), basal afferents in CA1 (Schaffer collaterals and A/C), mossy fibers in CA3, and A/C in CA3. The remaining electrodes were used to record the evoked field potentials, and the corresponding orthodromic dendritic field excitatory postsynaptic potential (fEPSP) responses with the largest amplitude were analyzed.

Input/output (I/O) curves data for each selected stimulation site in each subfield of the hippocampus were collected. The amplitudes of the responses were measured, and the stimulation intensities were set to yield 30%–40% of the maximal responses at each site. For each subfield study, each afferent was sequentially stimulated with paired pulses (30 ms interval) every 30 s to record a stable baseline response. For the experiments utilizing the high-density MEAs, throughout the entire experiments, both afferents were stimulated sequentially at 30-second intervals. After a 10 min baseline recording, the hippocampal slice was perfused with ACSF containing 100 pM of E_2 (Sigma) for 145 min when utilizing the 8×8 MEA or 60 min when utilizing the high-density MEA. At the end of the experiment, another set of I/O curves was recorded at each stimulation site.

Analytical methods for 8×8 MEA

The amplitude of the orthodromic dendritic fEPSP was measured as the difference between the maximum and the minimum of the recorded field potential, and the initial slope was measured of each pulse. I/O curves for each selected stimulation site were constructed by normalizing the fEPSP amplitude to the pre-estrogen amplitude response at 100 μA (maximum stimulation intensity used). The time course of the amplitude and slope of the first response, the amplitude and slope of the second response, and the paired pulse ratio (i.e. the ratio of amplitudes or slopes of the second response over the first response) were averaged across at least five experiments. The baseline amplitude was set to 100%.

The change in the response amplitude over time was reported as a percentage change from the baseline values. Following analysis of the amplitude of the response, topographical maps were constructed based on the differential change in values of fEPSP amplitudes (μV) before and after E_2 exposure. The differential change of the response of each electrode was color-coded, and the values between electrodes were bi-cubically interpolated.

Analytical methods for 3×20 MEA

The amplitude of the orthodromic dendritic fEPSP of the first pulse was measured as the difference between the maximum and the minimum of the recorded field potential, and the initial slope was measured of the first pulse. The time course of the amplitude for each afferent stimulation and the time course of the slope for each afferent stimulation were averaged across a minimal of five experiments. The baseline amplitude was set to 100%. The change in the response amplitude and slope over time was reported as a percentage change from the baseline values. To distinguish the two fEPSPs evoked in CA3, the 20%–80% time rises of the fEPSPs evoked from mossy fiber stimulation and from A/C fiber stimulation were compared (Kapur et al., 1998), and current source density (CSD) analysis was done to confirm stratum lucidum as the location for short latency current sink and to confirm stratum radiatum as the location for the short latency current source generated in response to mossy fiber stimulation (Urban and Barrionuevo, 1996; Yeckel and Berger, 1998). The one-dimensional CSD at each site (x) was calculated using the following formula: $I_x = (E_{x-h} - 2E_x + E_{x+h})$, where I_x is the current at location x , h is the sampling distance (50 μm), E_x is the extracellular voltage at location x , E_{x-h} is the extracellular voltage at location $x-h$, and E_{x+h} is the extracellular voltage at location $x+h$ (see Gholmieh et al., 2005 for more method details and for a complete treatment of the theoretical basis of CSD analysis, see Freeman and Nicholson, 1975). After each experiment, a metabotropic Glu receptor (mGluR) II agonist 2-(2,3-dicarboxycyclopropyl) glycine (DCG-IV) (1 μM) was added to the bath to confirm mossy fiber stimulation (Yoshino et al., 1996). Experiments in which DCG-IV did not diminish the mossy fiber response were discarded. A repeated measures ANOVA followed by Student-Newman-Keuls post hoc analysis was used to determine statically significant differences between baseline fEPSPs and post- E_2 fEPSPs.

RESULTS

CA1 stimulation

Using a paired pulse stimulation paradigm, E_2 induced an immediate yet gradual increase in the amplitude of the evoked fEPSP in CA1. Fig. 1A–1,2,3 shows a hippocampal slice stimulated at CA1 with the corresponding recorded fEPSPs pre- and post- E_2 treatment. Fig. 1B shows a representative pre- E_2 I/O curve and the potentiated post- E_2 I/O curve. Time course analysis of fEPSP amplitudes evoked by the first and the second pulse indicated that the fEPSP amplitude began to increase five to 10 minutes following addition of E_2 (Fig. 1C and 1D). At 145 min following E_2 exposure, the amplitude and slope of the first pulse fEPSP in CA1 was significantly increased by 20%±3% ($F(1,4)=4.33$, $P<0.01$) and 22%±7% ($F(1,4)=9.26$, $P<0.05$), respectively. E_2 potentiation of the fEPSP persisted for the second pulse with the amplitude and the slope of the fEPSP increased by 29%±5% ($F(1,4)=26.50$, $P<0.01$) and 27%±13% ($F(1,4)=9.26$, $P<0.05$), respectively (Fig. 1F and 1G). The paired pulse ratio of fEPSP amplitudes insignificantly increased from 180% to 190%

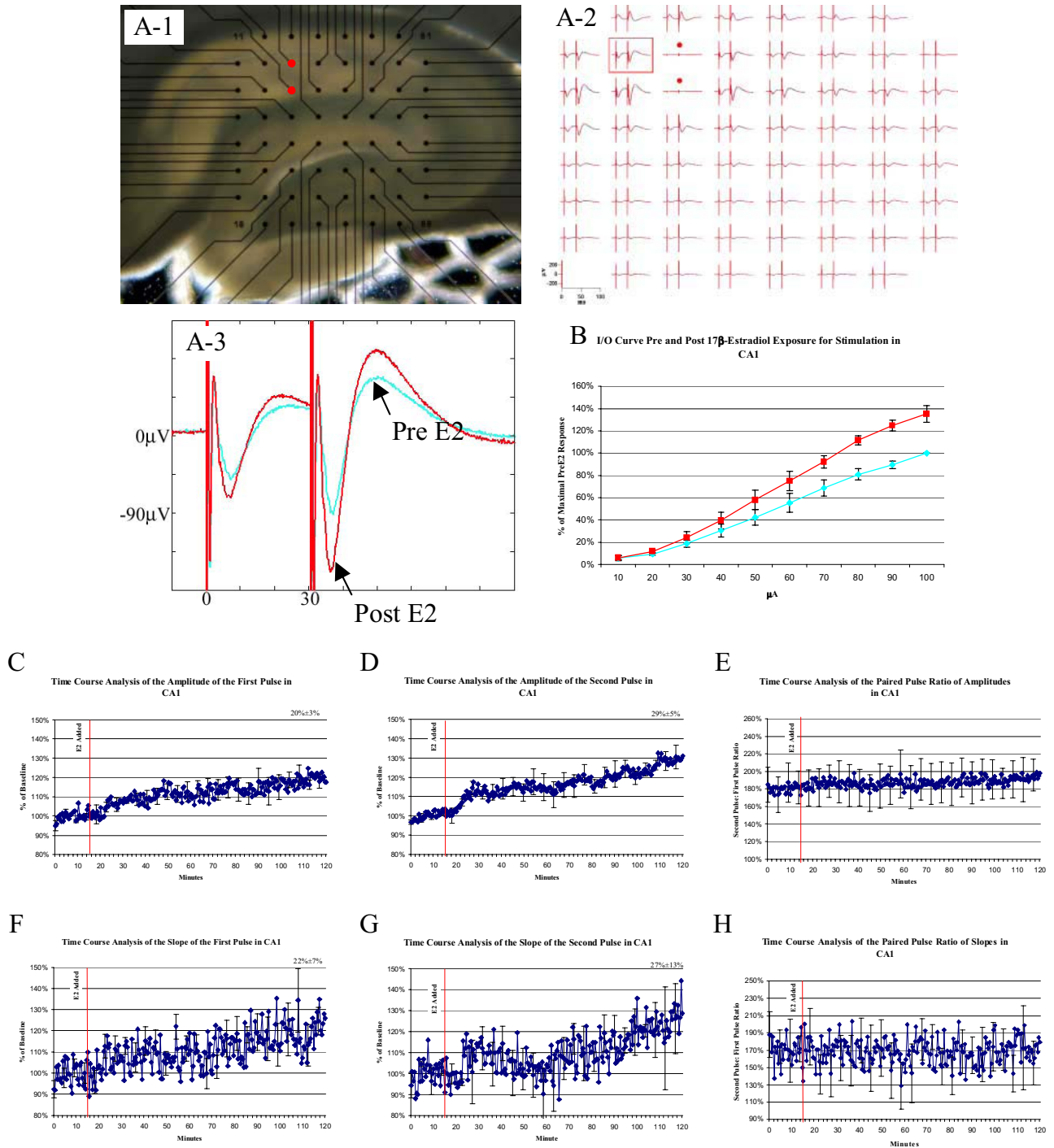


Fig. 1. E₂ potentiation of the paired pulse response following stimulation in CA1. (A) A representative experiment (one of five) demonstrating E₂-induced potentiation of fEPSPs stimulated in CA1. (A1) Hippocampal slice was placed on top of the MEA and aligned to allow simultaneous recording and stimulation of each of the three major subfields. The stimulation (red dots) consisted of two biphasic currents (100 μ s per phase, 30 ms ISI) in CA1. (A2) A representative overlay of fEPSPs was taken during the baseline collected prior to E₂ application (green) and 145 min following E₂ application (red) for each electrode. (A3) An orthodromic dendritic fEPSP from A2 (red box) is enlarged with waveforms taken before E₂ application (green) and the enhanced response observed after 145 min of E₂ application (red). (B) The I/O curve analysis before (green) and after (red) estrogen exposure shows the estrogen-induced potentiation on paired pulse stimulation in CA1. (C–H) Time course analyses of estrogenic potentiation of amplitudes and slopes. The time course analyses of the amplitude of the first pulse and second pulse in CA1 show that E₂ potentiated with an initial rapid enhancement of the fEPSPs and with a final enhancement of (C) 20% \pm 3% ($P < 0.01$) and (D) 29% \pm 5% ($P < 0.01$), respectively, while E₂ had no significant effect on the (E) paired pulse ratio of amplitude (185%). The time course analyses of the slope of the first pulse and second pulse in CA1 show that E₂ potentiated with an initial rapid enhancement of the fEPSPs and with a final enhancement of (F) 22% \pm 7% ($P < 0.05$) and (G) 27% \pm 13% ($P = 0.143$), respectively, while E₂ had no significant effect on the (H) paired pulse ratio of slope (170%). The red line indicates when estrogen was introduced into the bath. The error bars represent \pm S.E.M. and are shown for every fifth sweep in order to preserve clarity.

(Fig. 1E) whereas the paired pulse ratio of the slopes remained relatively constant at 170% (Fig. 1H). Fig. 4A shows two sets of topographical maps of the fEPSP amplitudes prior to and following E_2 exposure.

DG stimulation

Estrogen induced an increase in amplitude of fEPSP evoked in DG by paired pulse stimulus. Fig. 2A_{-1,2,3} shows a hippocampal slice stimulated at the DG with the corresponding recorded pre- E_2 and post- E_2 fEPSPs. Fig. 2B shows the pre- E_2 I/O curve and the potentiated post- E_2 I/O curve. At 145 min following E_2 exposure, the amplitude and slope of the first pulse fEPSP in DG significantly increased by $15\% \pm 4\%$ ($F(1,4)=10.88$, $P<0.05$) and $17\% \pm 5\%$ ($F(1,4)=11.14$, $P<0.05$), respectively (Fig. 2C and 2D). E_2 potentiation of the fEPSP persisted for the second pulse with the amplitude and the slope of the fEPSP increased by $7\% \pm 3\%$ ($F(1,4)=5.68$, $P=0.08$) and $9\% \pm 5\%$ ($F(1,4)=2.88$, $P=0.165$), respectively (Fig. 2F and 2G). The paired pulse ratio of the amplitudes decreased from 170% to 140% (Fig. 2E) while the paired pulse ratio of the slopes decreased from 115% to 100% (Fig. 2H). Because of the large variability, neither of these changes was statistically significant. Fig. 4B shows two sets of topographical maps—pre- E_2 exposure and post- E_2 exposure—generated by analysis of the amplitudes.

CA3 stimulation

Similar to CA1, estrogen induced an increase in amplitude of fEPSP evoked in CA3 by paired pulse stimulus. Fig. 3A_{-1,2,3} shows a hippocampal slice stimulated at CA3 with the corresponding recorded pre- E_2 and post- E_2 fEPSPs. Fig. 3B shows the pre- E_2 I/O curve and the post- E_2 -potentiated I/O curve. At 145 min following E_2 exposure, the amplitude and slope of the first pulse fEPSP in CA3 were significantly increased by $15\% \pm 4\%$ ($F(1,6)=10.90$, $P<0.05$) and $19\% \pm 5\%$ ($F(1,6)=18.42$, $P<0.01$), respectively (Fig. 3C and 3D). E_2 potentiation of the fEPSP persisted for the second pulse with the amplitude and the slope of the fEPSP increased by $13\% \pm 3\%$ ($F(1,6)=14.58$, $P<0.01$) and $10\% \pm 3\%$ ($F(1,6)=14.06$, $P<0.05$), respectively (Fig. 3F and 3G). The paired pulse ratio of the amplitude insignificantly decreased from 150% to 140% (Fig. 3E) while the paired pulse ratio of the slope remained relatively constant at 150% (Fig. 3H). It is interesting to note that in contrast to CA1 that exhibited potentiation within 10 min of E_2 exposure, the enhancement of fEPSP in CA3 was apparent at approximately 20 minutes after the addition of E_2 . Fig. 4C shows two sets of topographical maps—pre- E_2 exposure and post- E_2 exposure—generated by analysis of the amplitudes.

High-density array analysis of CA1

To determine the impact of E_2 on synaptic transmission within CA1 layers, high-density MEAs were constructed to record from multiple points along the dendritic tree of pyramidal cells, spanning basal and apical zones. E_2 induced a rapid increase in amplitude of the fEPSP evoked in basal

and apical dendrites in CA1. Fig. 5A_{-1,2} shows a hippocampal slice stimulated at CA1 with the corresponding recorded fEPSPs pre- and post- E_2 treatment. Time course analyses of the amplitudes for basal and apical fEPSP responses were consistent with those we observed using the lower density MEA with amplitudes increasing within five to 10 minutes following addition of E_2 (Fig. 5B and 5D). Following 60 min of E_2 exposure, fEPSPs amplitudes of basal afferent stimulation response in CA1 significantly increased by $10\% \pm 2\%$ ($F(1,4)=15.89$, $P<0.05$) while the fEPSP of the apical afferent stimulation response increased by $7\% \pm 2\%$ ($F(1,4)=12.18$, $P<0.05$). The slope of the fEPSPs similarly increased following basal stimulation in CA1 by $12\% \pm 3\%$ ($F(1,4)=13.42$, $P<0.05$) while the fEPSP of the apical stimulation increased by $9\% \pm 3\%$ ($F(1,4)=7.58$, $P<0.05$) (Fig. 5C and 5E). Each of the pathway's potentiations stabilized 40 min after E_2 onset at a level comparable to that reached within the same time by the less specific stimulation with the lower density MEA, which had yielded potentiation that kept rising further for two hours.

High-density array analysis of CA3

To determine the impact of E_2 on synaptic transmission within CA3 synaptic zones, we used high-density MEAs that spanned CA3 basal and apical dendritic zones with several electrodes in each region. Fig. 6A_{1,2} shows a hippocampal slice with a high-density CA3 array with stimulation electrodes for activation of mossy fibers and A/C fibers with the corresponding recorded pre- E_2 and post- E_2 fEPSPs. Following 60 min exposure to E_2 , the amplitude of the mossy fiber fEPSP was significantly potentiated by $15\% \pm 3\%$ ($F(1,4)=35.319$, $P<0.01$) (Fig. 6B), and the amplitude of the A/C fiber fEPSP was significantly potentiated by $31\% \pm 13\%$ ($F(1,4)=5.410$, $P<0.05$) (Fig. 6D). The slope of the mossy fiber fEPSP was significantly potentiated by $18\% \pm 6\%$ ($F(1,4)=9.984$, $P<0.05$) (Fig. 6C) whereas the slope of the fEPSP from A/C fiber stimulation was potentiated by $40\% \pm 15\%$ ($F(1,4)=6.718$, $P<0.05$) (Fig. 6E). The difference between slope and amplitude measurements could be due to the apparition of population spikes as the responses potentiated. The population spike would decrease the apparent fEPSP amplitude without affecting the initial slope measurement. To ensure that only mossy fibers were stimulated, a CSD analysis was conducted to determine current sinks and sources. This analysis confirmed previous reports that the current sink occurs at the stratum lucidum while the current source occurs at the stratum radiatum (Fig. 7) (Urban and Barrionuevo, 1996; Yeckel and Berger, 1998). Further, the fEPSP 20%–80% rise time following mossy fiber stimulation was 2.74 ± 0.45 ms while the A/C stimulated fEPSP 20%–80% rise time was 5.00 ± 0.60 ms. Our observed rise times for both mossy fibers and A/C fiber stimulated fEPSPs are consistent with previously reported rise times (Kapur et al., 1998). Finally, DCG-IV application eliminated the entire mossy fiber response while not affecting responses induced by A/C stimulation.

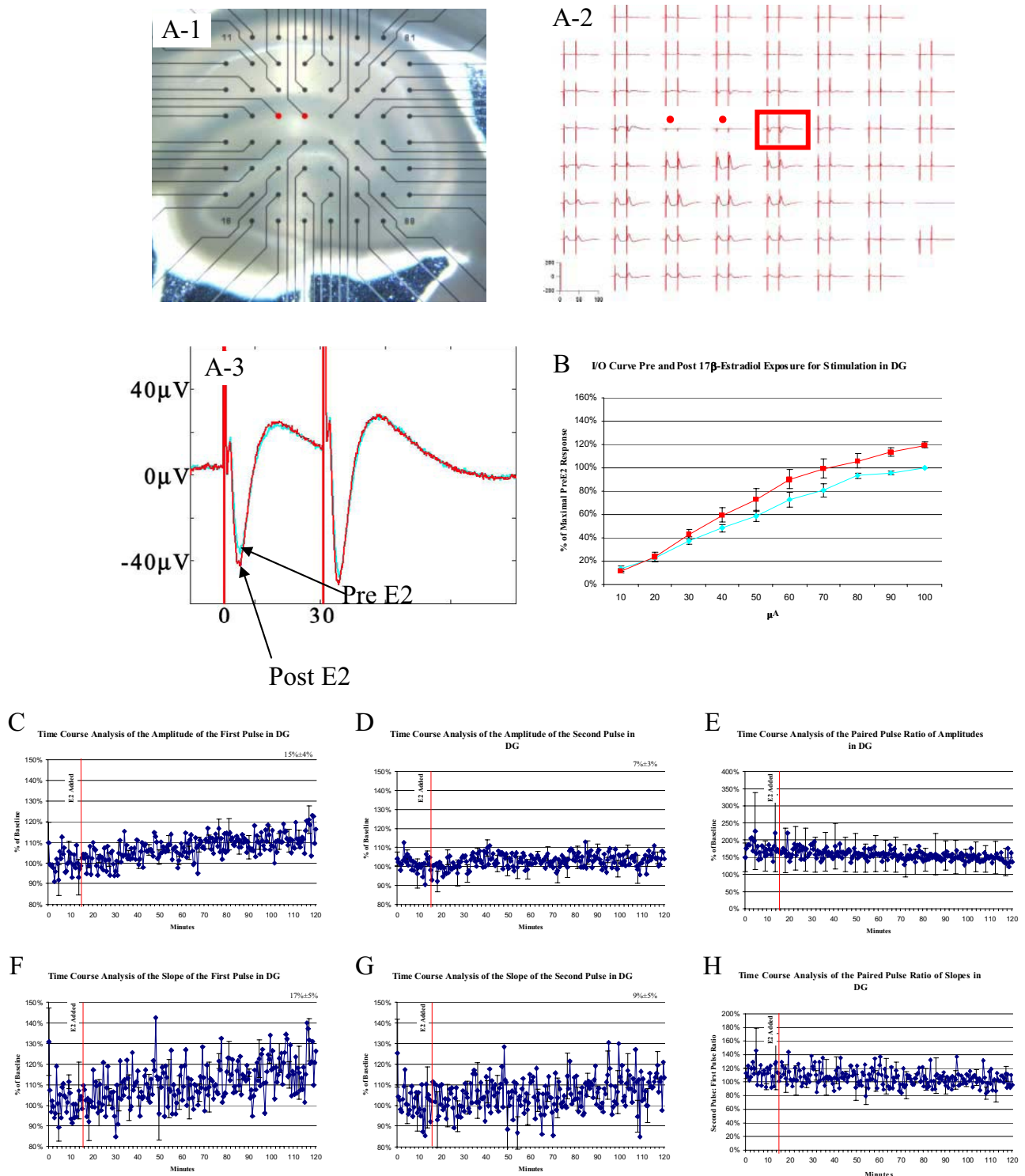


Fig. 2. E₂ potentiation of the paired pulse response following stimulation in DG. (A) A representative experiment (one of five) demonstrating E₂-induced potentiation of fEPSPs stimulated in DG. (A1) Hippocampal slice was placed on top of the MEA and aligned to allow simultaneous recording and stimulation of each of the three major subfields. The stimulation (red dots) consisted of two biphasic currents (100 μ s per phase, 30 ms ISI) in DG. (A2) A representative overlay of fEPSPs was taken during the baseline collected prior to E₂ application (green) and 145 min following E₂ application (red) for each electrode. (A3) An orthodromic dendritic fEPSP from A2 (red box) is enlarged with waveforms taken before E₂ application (green) and the enhanced response observed after 145 min of E₂ application (red). (B) The IO curve analysis before (green) and after (red) estrogen exposure shows the estrogen-induced potentiation on paired pulse stimulation in DG. (C–H) Time course analyses of estrogenic potentiation of amplitudes and slopes. The time course analyses of the amplitudes of the first pulse and second pulse in DG show that E₂ potentiated with an initial rapid enhancement of the fEPSPs and with a final enhancement of (C) 15% \pm 4% (P <0.05) and (D) 7% \pm 3% (P =0.076), respectively, while E₂ has no statistical significant effect on the (E) paired pulse ratio of amplitude (ranging from 170%–140%). The time course analyses of the slopes of the first pulse and second pulse in DG show that E₂ potentiated with an initial rapid enhancement of the fEPSPs and with a final enhancement of (F) 17% \pm 5% (P <0.05) and (G) 9% \pm 5% (P =0.165), respectively, while E₂ has no statistical significant effect on (H) the paired pulse ratio of slope (ranging from 115%–100%). The red line indicates when estrogen was introduced into the bath. The error bars represent \pm S.E.M. and are shown for every fifth sweep in order to preserve clarity.

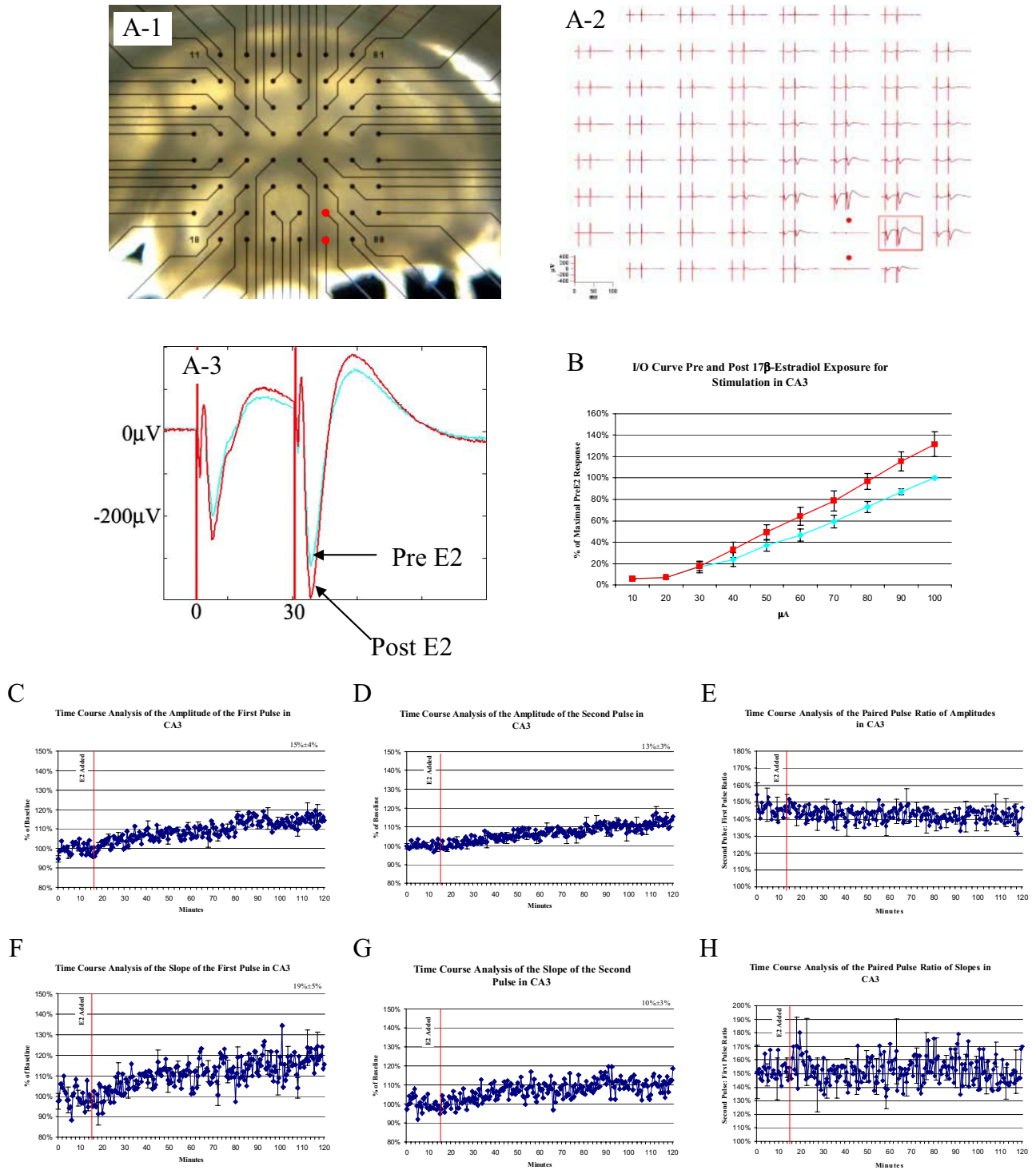


Fig. 3. E₂ potentiation of the paired pulse response following stimulation in CA3. (A) A representative experiment (one of five) demonstrating E₂-induced potentiation of fEPSPs stimulated in CA3. (A1) Hippocampal slice was placed on top of the MEA and aligned to allow simultaneous recording and stimulation of each of the three major subfields. The stimulation (red dots) consisted of two biphasic currents (100 μ s per phase, 30 ms ISI) in CA3. (A2) A representative overlay of fEPSPs was taken during the baseline collected prior to E₂ application (green) and 145 min following E₂ application (red) for each electrode. (A3) An orthodromic dendritic fEPSP from A2 (red box) is enlarged with waveforms taken before E₂ application (green) and the enhanced response observed after 145 min of E₂ application (red). (B) The I/O curve analysis before (green) and after (red) estrogen exposure shows the estrogen-induced potentiation on paired pulse stimulation in CA3. (C–H) Time course analyses of estrogenic potentiation of amplitudes and slopes. The time course analyses of the amplitude of the first pulse and second pulse in CA3 show that E₂ potentiated with an initial rapid enhancement of the fEPSPs and with a final enhancement of (C) 15% \pm 4% ($P < 0.05$) and (D) 13% \pm 3% ($P < 0.01$), respectively, while E₂ has no significant effect on (E) the paired pulse ratio of amplitude (145%). The time course analyses of the slope of the first pulse and second pulse in CA3 show that E₂ potentiated with an initial rapid enhancement of the fEPSPs and with a final enhancement of (F) 19% \pm 5% ($P < 0.01$) and (G) 10% \pm 3% ($P < 0.01$), respectively, while E₂ has no significant effect on (H) the paired pulse ratio of slope (150%). The red line indicates when estrogen was introduced into the bath. The error bars represent \pm S.E.M. and are shown for every fifth sweep in order to preserve clarity.

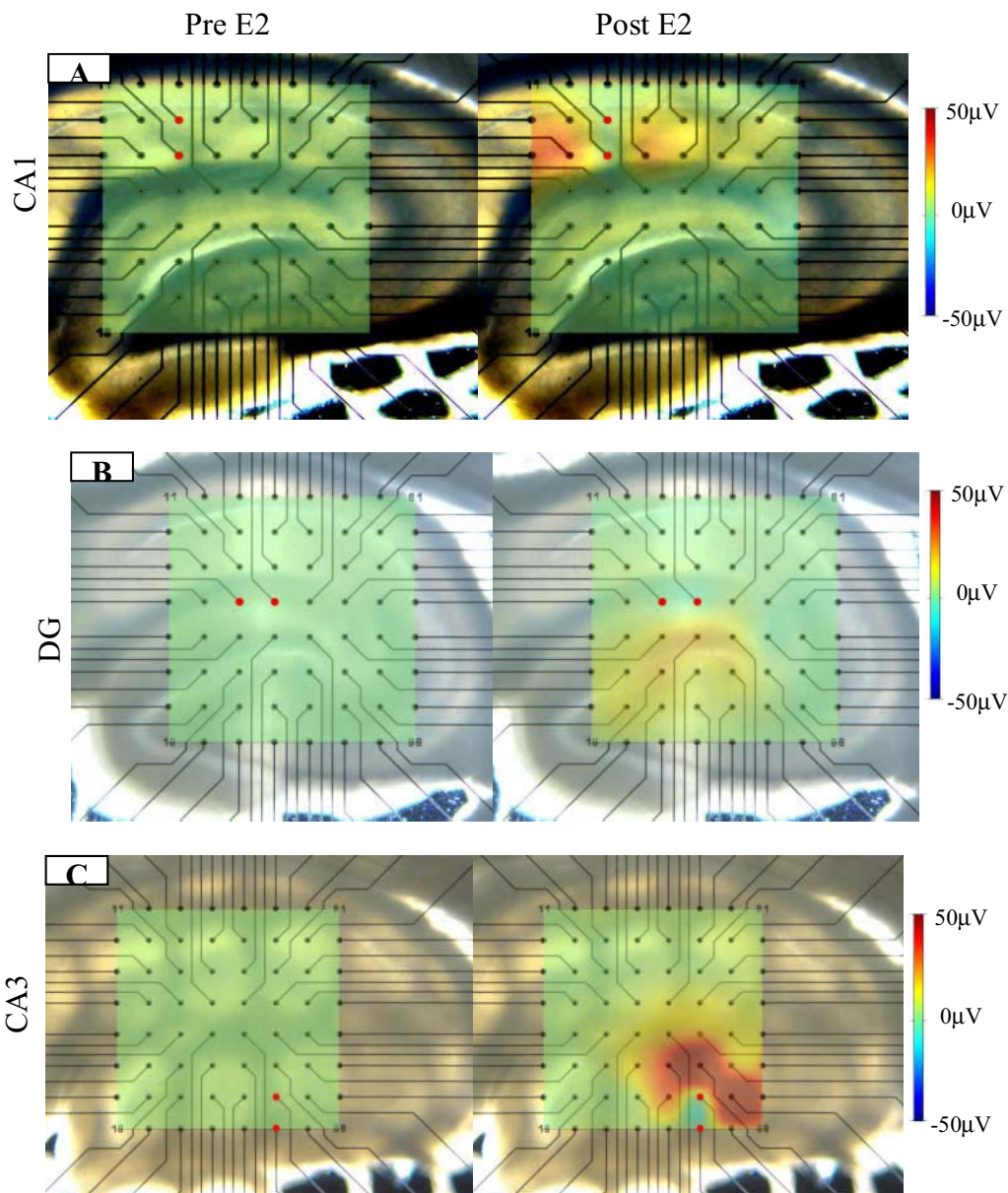


Fig. 4. Topographical activity analysis of E_2 potentiation of paired pulse response following stimulation in CA1, CA3, and DG. Analysis of the difference in fEPSP amplitudes (post E_2 exposure and baseline) was conducted for each recording electrode. Based on this analysis, the topographical maps were generated and overlaid onto the slice. The color scale for the differential topographical map is $+50 \mu\text{V}$ as red, $0 \mu\text{V}$ as green, and $-50 \mu\text{V}$ as blue. A. Stimulation in CA1. (B) Stimulation in CA3. (C) Stimulation in DG.

DISCUSSION

This study is the first characterization of E_2 regulation of the field excitatory postsynaptic potential evoked in the three major subfields of the hippocampus with an electrophysiological analysis of afferent fiber specificity within CA1 and CA3. First, we confirmed the rapid onset estrogenic potentiation of CA1 with fEPSPs potentiated in amplitude and slope which was apparent within 10 min and which gradually increased over the duration of the 145 min exposure to 100 pM of E_2 . Kumar and Foster (2002) reported that E_2 decreases the afterhyperpolarization in CA1 pyramidal cells, which allows for repetitive firing and which

may account for this persistent rise in fEPSP in the presence of E_2 observed in our current and previous analyses (Foy et al., 1999). Following validation of the MEA system to detect E_2 -inducible potentiation in CA1 similar to those previously reported (Foy and Teyler, 1983), we expanded the analysis to CA3 and DG. Both CA3 and DG exhibited significant potentiation of fEPSPs in amplitude and slope following E_2 exposure (Table 1).

The majority of previous analyses of estrogen regulation of synaptic transmission in hippocampus focused on CA1, specifically Schaffer collaterals' synapses onto stratum radiatum. Results of these analyses indicated

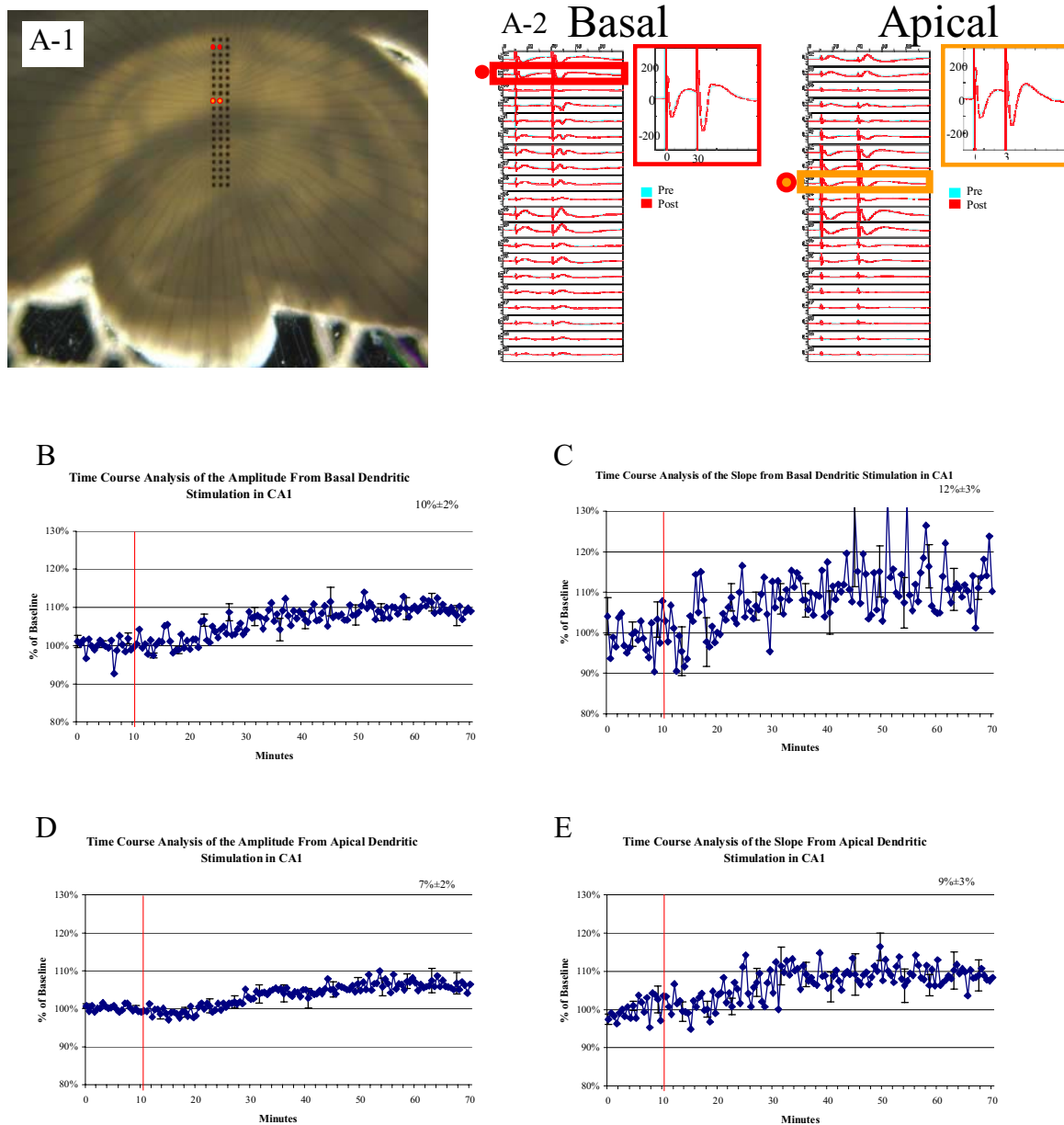


Fig. 5. E_2 potentiation of the fEPSP evoked in the basal and apical dendrites in CA1. (A) A representative experiment (one of five) demonstrating E_2 -induced potentiation of fEPSPs stimulated in the basal and apical dendrites in CA1. (A1) Hippocampal slice was placed on top of the high density MEA and aligned to allow simultaneous recording and stimulation of the apical and basal dendrites in CA1. The stimulation consisted of two biphasic currents ($100 \mu\text{s}$ per phase, 30 ms ISI) for the basal dendrites (red dots) and for the apical dendrites (orange dots) in CA1. (A2) A representative overlay of fEPSPs was taken during the baseline collected prior to E_2 application (green) and 60 min following E_2 application (red) for each electrode. (A3) The orthodromic dendritic fEPSPs from A-2 (box) are enlarged with waveforms taken before E_2 application (green) and the enhanced response observed after 60 min of E_2 application (red). (B–E) Time course analyses of estrogenic potentiation of amplitudes and slopes. Time course analyses of the amplitude and slope of the fEPSP evoked in the basal dendrites in CA1 show that E_2 potentiated with an initial rapid enhancement of the fEPSPs and with a final enhancement of (B) $10\% \pm 2\%$ ($P < 0.05$) in amplitude and (C) $12\% \pm 3\%$ ($P < 0.05$) in slope. Time course analyses of the amplitude and slope of the fEPSP evoked in the apical dendrites in CA1 show that E_2 potentiated with an initial rapid enhancement of the fEPSPs and with a final enhancement of (D) $7\% \pm 2\%$ ($P < 0.05$) in amplitude and (E) $9\% \pm 3\%$ ($P < 0.05$) in slope. The red line indicates when estrogen was introduced into the bath. The error bars represent \pm S.E.M. and are shown for every fifth sweep in order to preserve clarity.

that E_2 potentiated evoked fEPSPs in amplitude (overall cell excitability) and slope (synaptic transmission) (Gu and Moss, 1996, 1998; Foy et al., 1999; Gu et al., 1999) and further demonstrated that E_2 enhanced LTP through regulation of AMPA and NMDA channels (Foy et al., 1999; Bi et al., 2000, 2001; Kim et al., 2002). Through

the AMPA channels, E_2 enhanced fEPSPs via a G-protein-coupled receptor coupled to cAMP-dependent phosphorylation (Gu and Moss, 1996, 1998; Gu et al., 1999). Through the NMDA channels, E_2 leads to phosphorylation of the NMDA channel NR2 subunit following estrogen activation of Ca^{2+} /Src/MAPK/ERK signaling cascade (Bi et al., 2000,

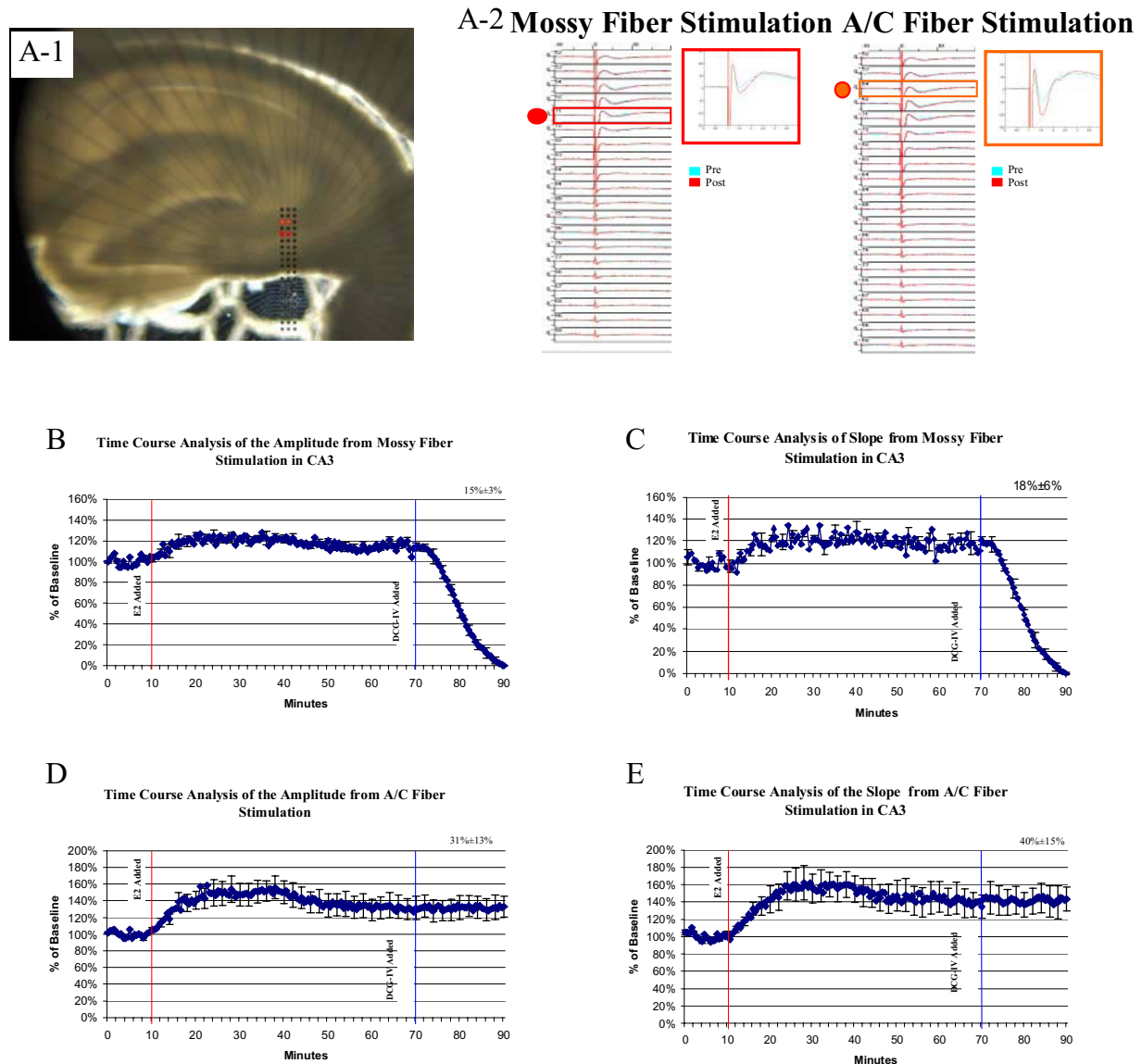


Fig. 6. E_2 potentiation of the fEPSP evoked by mossy fiber stimulation and by A/C stimulation in CA3. (A) A representative experiment (one of five) demonstrating E_2 -induced potentiation of fEPSPs evoked by mossy fiber stimulation and A/C fiber stimulation in CA3. (A1) Hippocampal slice was placed on top of the high density MEA and aligned to allow simultaneous recording and stimulation of the mossy fibers and A/C fibers in CA3. The stimulation consisted of two biphasic currents ($100 \mu\text{s}$ per phase, 30 ms ISI) for the mossy fibers (red dots) and for the A/C fibers (orange dots) in CA3. (A2) A representative overlay of fEPSPs was taken during the baseline collected prior to E_2 application (green) and 60 min following E_2 application (red) for each electrode. (A3) The orthodromic dendritic fEPSPs from A2 (box) are enlarged with waveforms taken before E_2 application (green) and the enhanced response observed after 60 min of E_2 application (red). (B–E) Time course analyses of estrogenic potentiation of amplitudes and slopes. Time course analyses of the amplitude and slope of the fEPSP evoked by mossy fiber stimulation in CA3 show that E_2 potentiated with an initial rapid enhancement of the fEPSPs and with a final enhancement of (B) $15\% \pm 3\%$ ($P < 0.05$) in amplitude and (C) $18\% \pm 6\%$ ($P < 0.05$) in slope. Time course analyses of the amplitude and slope of the fEPSP evoked by A/C fiber stimulation in CA3 show that E_2 potentiated with an initial rapid enhancement of the fEPSPs and with a final enhancement of (D) $31\% \pm 13\%$ ($P < 0.05$) in amplitude and (E) $40\% \pm 15\%$ ($P < 0.05$) in slope. The red line indicates when estrogen was introduced into the bath. The blue line indicates when DCG-IV was introduced into the bath. The error bars represent \pm S.E.M. and are shown for every fifth sweep in order to preserve clarity.

2001; Kim et al., 2002; Nilsen et al., 2002). Moreover, our recent work has shown that E_2 -induces calcium influx through L-type calcium channels and is required for E_2 activation of the Src/ERK/CREB/Bcl-2 signaling cascade (Wu et al., 2005; Zhao et al., 2005). These mechanisms of estrogenic action could occur in CA3 where L-type calcium channels are abundant (Woodside et al.,

2004) and where the A/C fibers contain NMDA receptors (Siegel et al., 1994).

We used a paired pulse protocol that tests for postsynaptic and presynaptic mechanisms by the examination of short term plasticity dependent on presynaptic calcium buildup and vesicular priming and the changes in probability of release of vesicles (Zalutsky and Nicoll,

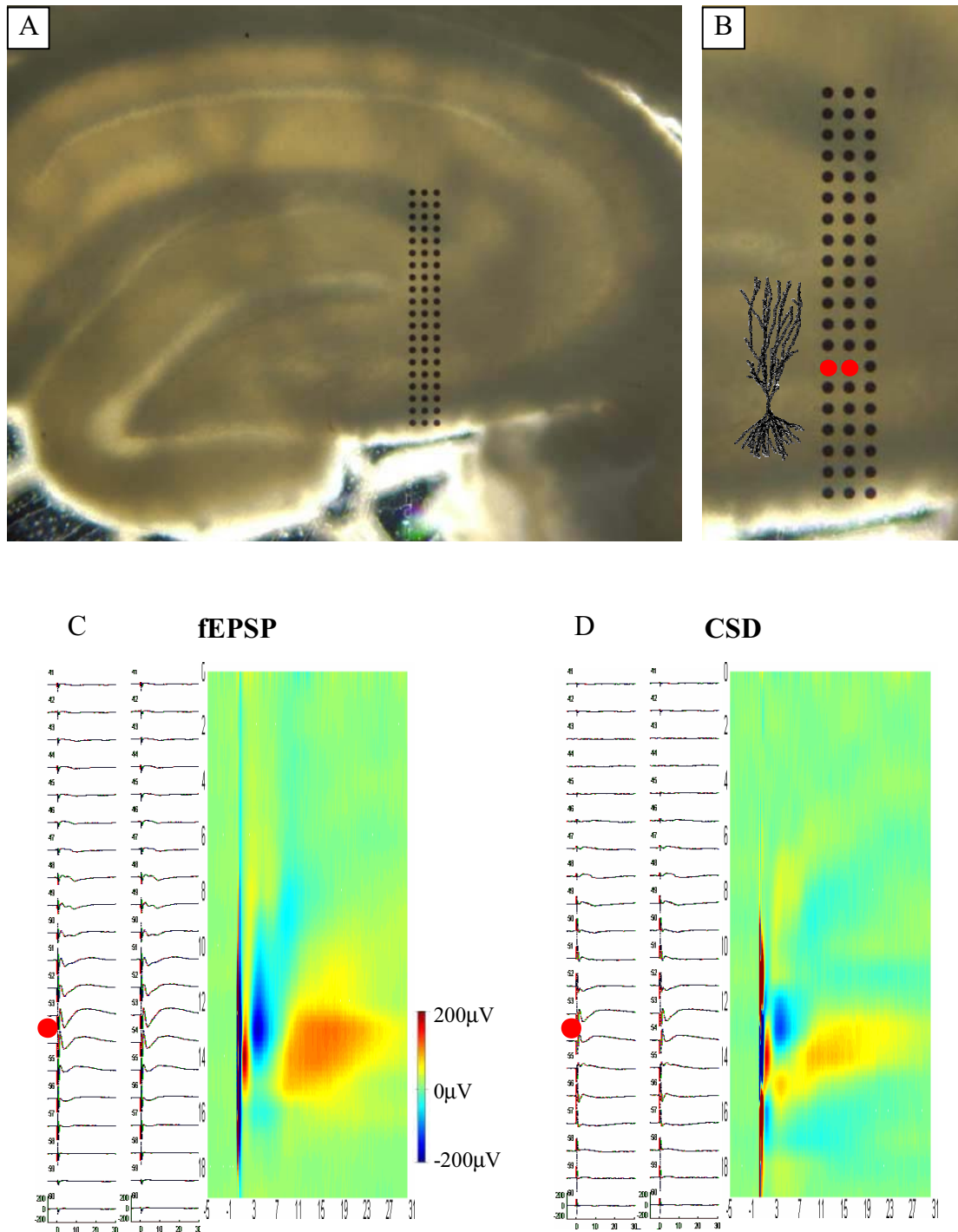


Fig. 7. CSD analysis from mossy fiber stimulation in CA3. A one dimensional CSD analysis of the fEPSPs recorded from the high-density MEA confirmed that fEPSP evoked from stimulating in the stratum lucidum was from mossy fiber stimulation. (A) The hippocampal slice was placed on top of the MEA and aligned so that the mossy fibers could be stimulated and the entire CA3 pyramidal neuron could be recorded. (B) An enlarged image of the high-density probe with a diagram of the CA3 pyramidal neuron. The two electrodes marked in red were used to stimulate the mossy fibers, and the non-stimulated column of electrodes was used to record. (C) Each recorded fEPSP in the grid contains the potential change under control conditions with a topographical map that color codes the exact voltage (μV) as a function of time (ms). (D) CSD analysis of the fEPSP shows the spatial and temporal distribution of current sinks ($-$ values) and current sources ($+$ values). This analysis confirms that the mossy fibers were stimulated since a current sink was found in stratum lucidum and a current source was found in stratum radiatum.

1990; Thiels et al., 1994; Ghaffari-Farazi et al., 1999). Results of our analyses indicated no significant change

in the paired pulse ratio for either fEPSPs amplitude or slope evoked in all three subfields. Potentiation of fEPSPs

Table 1. Baseline enhancement of fEPSP amplitude and slope at first stimulation pulse

Site	Enhancement	
	Amplitude	Slope
DG	15%±4%*	17%±5%*
CA3	15%±4%*	19%±5%**
CA1	20%±3%**	22%±7%*

Values are means±S.E.M. * $P<0.05$, ** $P<0.01$.

following E_2 exposure without a change in the paired pulse ratios is consistent with a postsynaptic mechanism that is consistent with previously reported postsynaptic mechanisms of estrogen action (Wong and Moss, 1992; Foy et al., 1999; Brinton, 2001). However, a presynaptic mechanism cannot be ruled out since estrogen attenuates the inhibition by the GABA_A channels by a presynaptic mechanism (Rudick and Woolley, 2001; Rudick et al., 2003) in CA1.

To investigate the site of estrogen potentiation, we conducted detailed analyses of the afferent pathways of CA1 and CA3. Results of the current analyses demonstrate that in CA1, the magnitude of E_2 -induced fEPSP potentiations following apical and basal dendritic stimulations was comparable to each other, although stabilizing at half the potentiation observed with the less selective stimulation elicited by the lower density MEA. In CA1, the basal dendritic afferents are derived from the Schaffer collaterals and A/C fibers while the apical dendrites are primarily innervated by Schaffer collaterals (Swanson et al., 1978). Moreover, there are different ratios of inhibitory and excitatory synapses formed on the CA1 pyramidal neuron in different strata in CA1. In stratum oriens, 3% of the synapses formed on the pyramidal neurons are inhibitory while 18% of synapses in the stratum radiatum are inhibitory (Megias et al., 2001). However, the different afferent stimulation did not result in significant differences in estrogenic potentiation in CA1, suggesting that the observed potentiation is due to post-synaptic mechanisms.

In contrast, in CA3, E_2 -induced potentiation of A/C fiber stimulation was found to be greater than that induced by mossy fiber stimulation. Furthermore, the selective fiber stimulation led to potentiation that stabilized in 10–15 min and was larger than the potentiation induced by the non-selective stimulation through the lower density MEA. In CA3, two major excitatory afferents for the pyramidal cells are the mossy fibers and the A/C fibers. A major difference between the two afferents is that the mossy fibers did not express NMDA receptors while the A/C fibers do. Moreover, class D voltage dependent L-type calcium channels are found on the soma and proximal apical dendrites of pyramidal cells in CA3 (Hell et al., 1993) while class C L-type calcium channels are found on the entire CA3 pyramidal neuron (Hell et al., 1996). Therefore, the combination of NMDA receptors and L-type calcium channels on the A/C fiber synapses in CA3 could account for the observed potentiation.

Relationship of E_2 potentiation of fEPSPs and estrogen receptor distribution

We sought to relate our findings to the distribution of estrogen receptors, ER α and ER β , in the hippocampus. Since estrogen potentiated EPSPs in wild-type mice and in ER α knockout mice (Gu et al., 1999; Fugger et al., 2001), it is suggested that E_2 -potentiation of fEPSPs in CA1 at least does not require ER α . CA3 expresses a relatively high level of ER β (Shughrue et al., 1997; Shughrue and Merchenthaler, 2000; Zhang et al., 2002; Mitra et al., 2003). The greatest E_2 -induced potentiation occurred following A/C fiber stimulation in CA3 in which expresses both NMDA receptors and ER β (Fig. 8). Our recent work has shown that ER β is equally efficacious as ER α on several measures of estrogen receptor function (Zhao et al., 2004).

The potential significance of E_2 potentiation of CA3 and of A/C fibers in particular can be gleaned from the anatomical and functional complexity of CA3 (Laurberg and Sorensen, 1981; Fig. 9A). At the anatomical level, CA3 mossy fibers participate in the trisynaptic pathway while the A/C fibers send ipsilateral projections to reinforce connections and contralateral projections to unify the two hippocampi of the brain with contralateral projections forming synapses at the same area from where they were sent (Swanson et al., 1978). A/C fibers integrate information along the long axis of the hippocampus (Amaral and Witter, 1989), that can assist the dentate to overcome resistance to discharge (Stringer and Lothman, 1989; Stringer et al., 1989), and unify hippocampi function (Gloor et al., 1993).

CA3 pyramidal neurons express the highest density of ER β , receive input from mossy fibers and A/C fibers, and express both L-type calcium channels and NMDA channels (Hell et al., 1993, 1996). These two calcium channels participate in different phases of memory function with NMDA channels required for memory acquisition while L-type calcium channels are necessary for memory retention (Grover and Teyler, 1990, 1992; Teyler et al., 1995; Nakazawa et al., 2002; Woodside et al., 2004). Consistent with these functional analyses, our recent work has shown that E_2 -induces calcium influx through L-type calcium channels and is required for E_2 activation of the Src/ERK/CREB/Bcl-2 signaling cascade (Wu et al., 2005; Zhao et al., 2005). E_2 -induced Src/ERK signaling cascade is required for phosphorylation of the NMDA receptor and ultimately enhanced LTP and morphogenesis (Akopian et al., 2003; Wu et al., 2005; Zhao et al., 2005). Our *in vitro* data indicate that E_2 activation of calcium influx is specific for calcium conductance through L-type channels and not via N, T or P, Q, R types of channels (Wu et al., 2005). These data are consistent with observations from Thompson and colleagues (Akopian et al., 2003) who have shown that E_2 enhancement of LTP in hippocampal slices is dependent upon voltage dependent calcium channels.

Significance of E_2 potentiation of A/C fibers in CA3

Increasing evidence indicates that CA3 can serve as an associative memory network due to the sparse connectivity of

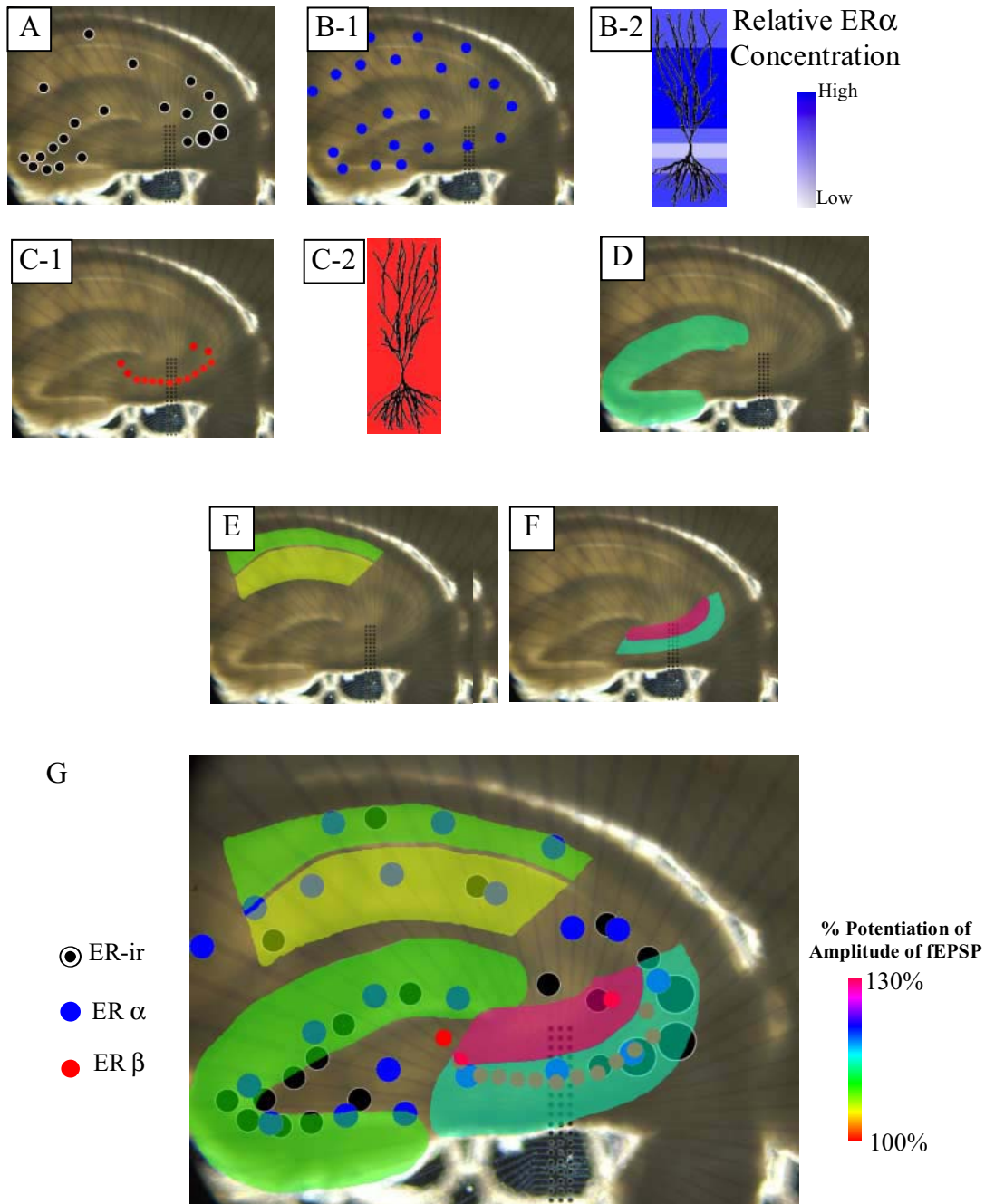
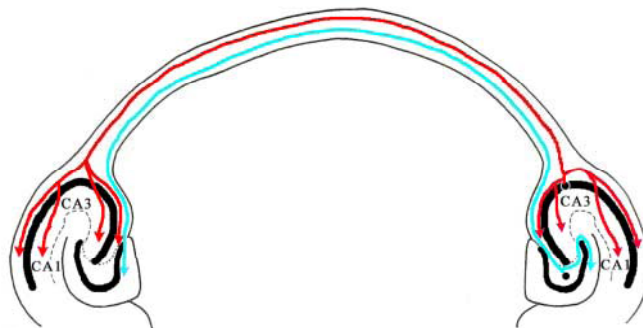


Fig. 8. Estrogen receptor and potentiation map. Comparative depiction of E_2 receptor binding in hippocampus (Shughrue and Merchenthaler, 2000; Milner et al., 2001; Mitra et al., 2003) and potentiation of the fEPSP within DG, CA3 and CA1 regions of the hippocampal slice. (A) Map of I-125 estrogen binding in the hippocampus (Shughrue and Merchenthaler, 2000). (B1) Map of ER α labeling in hippocampus by four ER α antibodies (Milner et al., 2001). (B2) Detailed ER α map of CA3 pyramidal neuron as detected by ER α antibodies (Milner et al., 2001). (C1) Map of ER β labeling in hippocampus as detected by ER β antibody 80424 (Mitra et al., 2003). (C2) Detailed ER β localization in CA3 pyramidal neuron as determined by ER β antibody 80424 (Mitra et al., 2003). (D) DG evoked fEPSP amplitude potentiation map after 60 min exposure to E_2 . (E) CA1 evoked fEPSP amplitude potentiation map after 60 min exposure to E_2 . (F) CA3 evoked fEPSP amplitude potentiation map after 60 min exposure to E_2 . (G) Superimposition of maps of estrogen receptors and E_2 -induced potentiation. Though estrogen potentiated all of the fEPSP evoked in all three subfields of the hippocampus, the greatest potentiation occurred at CA3 at the A/C fiber stimulation.

mossy fibers (0.005%) and its denser connectivity of associational fibers (2%) (Traub and Miles, 1991; Rolls, 1996; O'Reilly et al., 1998; Gonzales et al., 2001). In an associative memory network, memories are proposed to be stored

through modification of synaptic strengths within the network (Liaw and Berger, 1996). The associative fibers are modified in a NMDA receptor-dependent manner to reinforce and strengthen connections between coactive neurons within the

A



B

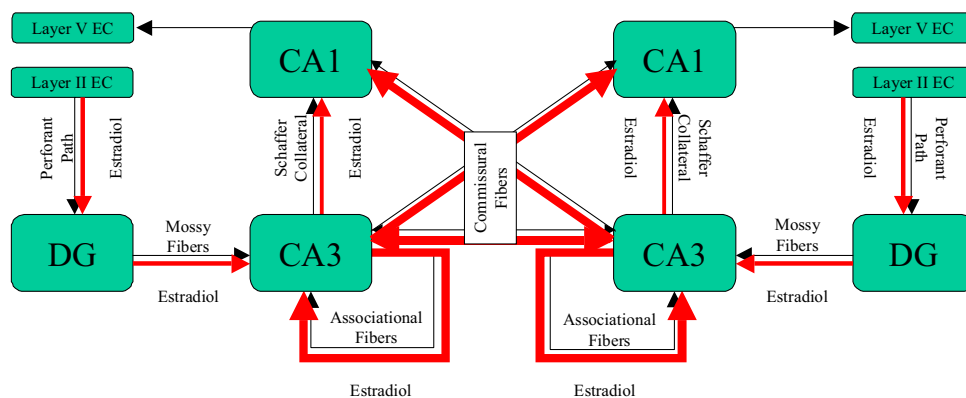


Fig. 9. A/C fiber tracts and estrogen potentiation map in the hippocampus. (A) Schematic diagram of the A/C fibers (adapted from (Laurberg and Sorensen, 1981)). The red lines are the A/C fibers associated with the pyramidal cells. The associational fibers form connections ipsilaterally while the commissural fibers form connections contralaterally. The green lines are the A/C fibers associated with the granule cells. (B) Schematic diagram of the tri-synaptic pathway in hippocampal slice (adapted from (Nakazawa et al., 2002)). The entorhinal cortex (EC) provides the input to the DG through the perforant pathway. The granule cells from the DG send mossy fibers to the CA3 pyramidal cells, which extend their axons (Schaffer collaterals) to the CA1 pyramidal cells. The other sets of fibers emanating from CA3 form excitatory recurrent collaterals within CA3 (associational fibers) and form contralateral connections to CA3 and CA1 (commissural fibers). Estrogen has been demonstrated to potentiate fEPSP evoked by the perforant path, mossy fibers, Schaffer collaterals and A/C fibers in CA3. (Red arrows demonstrate where there is an estrogen-induced potentiation on synaptic transmission in the hippocampus.) Functionally, we propose that estrogen-induced potentiation of each component of the trisynaptic pathway leads to an increase in the absolute number of items that can be stored in the memory network. The selective enhancement of the A/C fibers system of CA3 suggests that estrogen enhances the retrieval function of CA3 such that fewer elements (i.e. a partial representation) of a memory would be required for the whole memory to be retrieved.

network (Nakazawa et al., 2002). The working model of associative connections/memory proposes that, entire memory patterns can be retrieved from partial representations of the memory and is manifested as pattern completion (Traub and Miles, 1991; Rolls, 1996; O'Reilly et al., 1998; Nakazawa et al., 2002). Lack of NMDA receptors leads to impairment of pattern completion capability (Nakazawa et al., 2002). Impairment of association fiber function via decrement or lack of NMDA receptors is consistent with a crucial role of associational fibers for the pattern completion property of associative memory recall.

Estrogen potentiation of the fEPSP of each component of the trisynaptic pathway of the hippocampus suggests that estrogen regulates hippocampal function broadly while selectively enhancing the function of CA3 A/C fiber system (Fig. 9B). Functionally, we propose that estrogen-induced potentiation of each component of the trisynaptic

pathway leads to an increase in the absolute number of items that can be stored in the memory network. Further, the selective enhancement of the A/C fibers system of CA3 suggests that estrogen enhances the retrieval function of CA3 such that fewer elements (i.e. a partial representation) of a memory would be required for the whole memory to be retrieved. If this hypothesis is correct, then the corollary should be true: that a deficiency in estrogen would lead to a requirement for a greater number of the elements (larger representation) of the memory to retrieve the entire memory. This hypothesis is readily testable in both animal and human behavioral analyses.

CONCLUSION

To summarize, data presented herein demonstrate that estrogen significantly potentiated the fEPSPs within each of the

subfields of the hippocampal trisynaptic pathway (perforant path, mossy fibers, and Schaffer collaterals). Of particular importance is the discovery that the greatest potentiation by E_2 occurred at the A/C fiber synapse in CA3. Local potentiation of synaptic transmission within each of the nodes of the trisynaptic pathway coupled with the morphogenic effects of E_2 could transform these local nodes of potentiation to a global network of potentiation with the A/C fibers in CA3 enhancing memory retrieval through auto-associative memory and pattern completion. These findings extend our understanding of estrogen regulation of hippocampal synaptic activity to each subfield of the hippocampal trisynaptic pathway. More importantly, the discovery that the greatest impact of E_2 is on the A/C fibers within CA3 provides a mechanistic framework upon which to test hypotheses relevant to the behavioral consequences of estrogen exposure in the hippocampus. For example, E_2 potentiation of A/C fibers in CA3 of the hippocampus would predict that memory tasks that rely on retrieval of information based on partial representations of the memory would be sensitive to the absence or presence of E_2 .

Acknowledgments—This work was supported by National Institutes of Aging (PO1 AG1475; Project 2) to R.D.B. and T.W.B. and by the Kenneth T. and Eileen L. Norris Foundation and the L.K. Whittier Foundation to R.D.B.

REFERENCES

- Akopian G, Foy MR, Thompson RF (2003) 17 beta-Estradiol enhancement of LTP involves activation of voltage-dependent calcium channels. Program No. 255.2. 2003 Abstract Viewer/Itinerary Planner. Washington, DC: Society for Neuroscience, 2003. Online.
- Amaral DG, Witter MP (1989) The three-dimensional organization of the hippocampal formation: a review of anatomical data. *Neuroscience* 31:571–591.
- Bi R, Broutman G, Foy MR, Thompson RF, Baudry M (2000) The tyrosine kinase and mitogen-activated protein kinase pathways mediate multiple effects of estrogen in hippocampus. *Proc Natl Acad Sci U S A* 97:3602–3607.
- Bi R, Foy MR, Vouimba RM, Thompson RF, Baudry M (2001) Cyclic changes in estradiol regulate synaptic plasticity through the MAP kinase pathway. *Proc Natl Acad Sci U S A* 98:13391–13395.
- Brinton RD (2001) Cellular and molecular mechanisms of estrogen regulation of memory function and neuroprotection against Alzheimer's disease: recent insights and remaining challenges. *Learn Mem* 8:121–133.
- Brinton RD, Tran J, Proffitt P, Montoya M (1997a) 17 beta-Estradiol enhances the outgrowth and survival of neocortical neurons in culture. *Neurochem Res* 22:1339–1351.
- Brinton RD, Proffitt P, Tran J, Luu R (1997b) Equilin, a principal component of the estrogen replacement therapy premarin, increases the growth of cortical neurons via an NMDA receptor-dependent mechanism. *Exp Neurol* 147:211–220.
- Chiaia N, Foy M, Teyler TJ (1983) The hamster hippocampal slice: II. Neuroendocrine modulation. *Behav Neurosci* 97:839–843.
- Egert U, Schlosshauer B, Fennrich S, Nisch W, Fejt M, Knott T, Muller T, Hammerle H (1998) A novel organotypic long-term culture of the rat hippocampus on substrate-integrated multielectrode arrays. *Brain Res Brain Res Protoc* 2:229–242.
- Foy MR, Teyler TJ (1983) 17-alpha-Estradiol and 17-beta-estradiol in hippocampus. *Brain Res Bull* 10:735–739.
- Foy MR, Chiaia NL, Teyler TJ (1984) Reversal of hippocampal sexual dimorphism by gonadal steroid manipulation. *Brain Res* 321:311–314.
- Foy MR, Xu J, Xie X, Brinton RD, Thompson RF, Berger TW (1999) 17beta-Estradiol enhances NMDA receptor-mediated EPSPs and long-term potentiation. *J Neurophysiol* 81:925–929.
- Freeman JA, Nicholson C (1975) Experimental optimization of current source-density technique for anuran cerebellum. *J Neurophysiol* 38:369–382.
- Fugger HN, Kumar A, Lubahn DB, Korach KS, Foster TC (2001) Examination of estradiol effects on the rapid estradiol mediated increase in hippocampal synaptic transmission in estrogen receptor alpha knockout mice. *Neurosci Lett* 309:207–209.
- Ghaffari-Farazi T, Liaw J-S, Berger TW (1999) Consequence of morphological alterations on synaptic function. *Neurocomputing* 26–27:17–27.
- Gholmieh G, Soussou W, Han M, Ahuja A, Hsiao MC, Song D, Tanguay AR Jr, Berger TW (2005) Custom-designed high-density conformal planar multielectrode arrays for brain slice electrophysiology. *J Neurosci Methods* 2006:116–129.
- Gloor P, Salanova V, Olivier A, Quesney LF (1993) The human dorsal hippocampal commissure. An anatomically identifiable and functional pathway. *Brain* 116:1249–1273.
- Gonzales RB, DeLeon Galvan CJ, Rangel YM, Claiborne BJ (2001) Distribution of thorny excrescences on CA3 pyramidal neurons in the rat hippocampus. *J Comp Neurol* 430:357–368.
- Grover LM, Teyler TJ (1990) Two components of long-term potentiation induced by different patterns of afferent activation. *Nature* 347:477–479.
- Grover LM, Teyler TJ (1992) N-methyl-D-aspartate receptor-independent long-term potentiation in area CA1 of rat hippocampus: input-specific induction and preclusion in a non-tetanized pathway. *Neuroscience* 49:7–11.
- Gu Q, Moss RL (1996) 17 beta-Estradiol potentiates kainate-induced currents via activation of the cAMP cascade. *J Neurosci* 16:3620–3629.
- Gu Q, Moss RL (1998) Novel mechanism for non-genomic action of 17 beta-oestradiol on kainate-induced currents in isolated rat CA1 hippocampal neurones. *J Physiol* 506:745–754.
- Gu Q, Korach KS, Moss RL (1999) Rapid action of 17beta-estradiol on kainate-induced currents in hippocampal neurons lacking intracellular estrogen receptors. *Endocrinology* 140:660–666.
- Hell JW, Westenbroek RE, Breeze LJ, Wang KK, Chavkin C, Catterall WA (1996) N-methyl-D-aspartate receptor-induced proteolytic conversion of postsynaptic class C L-type calcium channels in hippocampal neurons. *Proc Natl Acad Sci U S A* 93:3362–3367.
- Hell JW, Westenbroek RE, Warner C, Ahljianian MK, Prystay W, Gilbert MM, Snutch TP, Catterall WA (1993) Identification and differential subcellular localization of the neuronal class C and class D L-type calcium channel alpha 1 subunits. *J Cell Biol* 123:949–962.
- Kapur A, Yeckel MF, Gray R, Johnston D (1998) L-type calcium channels are required for one form of hippocampal mossy fiber LTP. *J Neurophysiol* 79:2181–2190.
- Kim JS, Kim HY, Kim JH, Shin HK, Lee SH, Lee YS, Son H (2002) Enhancement of rat hippocampal long-term potentiation by 17 beta-estradiol involves mitogen-activated protein kinase-dependent and -independent components. *Neurosci Lett* 332:65–69.
- Kumar A, Foster TC (2002) 17beta-Estradiol benzoate decreases the AHP amplitude in CA1 pyramidal neurons. *J Neurophysiol* 88(2):621–626.
- Laurberg S, Sorensen KE (1981) Associational and commissural collaterals of neurons in the hippocampal formation (hilus fasciae dentatae and subfield CA3). *Brain Res* 212:287–300.
- Liaw JS, Berger TW (1996) Dynamic synapse: a new concept of neural representation and computation. *Hippocampus* 6:591–600.
- Loy R, Gerlach JL, McEwen BS (1988) Autoradiographic localization of estradiol-binding neurons in the rat hippocampal formation and entorhinal cortex. *Brain Res* 467:245–251.

- Megias M, Emri Z, Freund TF, Gulyas AI (2001) Total number and distribution of inhibitory and excitatory synapses on hippocampal CA1 pyramidal cells. *Neuroscience* 102:527–540.
- Milner TA, McEwen BS, Hayashi S, Li CJ, Reagan LP, Alves SE (2001) Ultrastructural evidence that hippocampal alpha estrogen receptors are located at extranuclear sites. *J Comp Neurol* 429:355–371.
- Mitra SW, Hoskin E, Yudkovitz J, Pear L, Wilkinson HA, Hayashi S, Pfaff DW, Ogawa S, Rohrer SP, Schaeffer JM, McEwen BS, Alves SE (2003) Immunolocalization of estrogen receptor beta in the mouse brain: comparison with estrogen receptor alpha [erratum appears in *Endocrinology*. 2003 Jul;144(7):2844]. *Endocrinology* 144:2055–2067.
- Nakazawa K, Quirk MC, Chitwood RA, Watanabe M, Yeckel MF, Sun LD, Kato A, Carr CA, Johnston D, Wilson MA, Tonegawa S (2002) Requirement for hippocampal CA3 NMDA receptors in associative memory recall. *Science* 297:211–218.
- Nilsen J, Chen S, Brinton RD (2002) Dual action of estrogen on glutamate-induced calcium signaling: mechanisms requiring interaction between estrogen receptors and src/mitogen activated protein kinase pathway. *Brain Res* 930:216–234.
- Nishio M, Kuroki Y, Watanabe Y (2004) Subcellular localization of estrogen receptor beta in mouse hippocampus. *Neurosci Lett* 355:109–112.
- O'Reilly RC, Norman K, McClelland JL (1998) A hippocampal model of recognition memory. In: *Advances in neural information processing systems* (Jordan MI, Kearns MJ, Solla SA, eds), pp 73–79. Cambridge, MA: MIT Press.
- Rolls ET (1996) A theory of hippocampal function in memory. *Hippocampus* 6:601–620.
- Rudick CN, Woolley CS (2001) Estrogen regulates functional inhibition of hippocampal CA1 pyramidal cells in the adult female rat. *J Neurosci* 21:6532–6543.
- Rudick CN, Gibbs RB, Woolley CS (2003) A role for the basal forebrain cholinergic system in estrogen-induced disinhibition of hippocampal pyramidal cells. *J Neurosci* 23:4479–4490.
- Shughrue PJ, Merchenthaler I (2000) Evidence for novel estrogen binding sites in the rat hippocampus. *Neuroscience* 99:605–612.
- Shughrue PJ, Lane MV, Merchenthaler I (1997) Comparative distribution of estrogen receptor-alpha and -beta mRNA in the rat central nervous system. *J Comp Neurol* 388:507–525.
- Siegel SJ, Brose N, Janssen WG, Gasic GP, Jahn R, Heinemann SF, Morrison JH (1994) Regional, cellular, and ultrastructural distribution of N-methyl-D-aspartate receptor subunit 1 in monkey hippocampus. *Proc Natl Acad Sci U S A* 91:564–568.
- Stringer JL, Lothman EW (1989) Maximal dentate gyrus activation: characteristics and alterations after repeated seizures. *J Neurophysiol* 62:136–143.
- Stringer JL, Williamson JM, Lothman EW (1989) Induction of paroxysmal discharges in the dentate gyrus: frequency dependence and relationship to afterdischarge production. *J Neurophysiol* 62:126–135.
- Swanson LW, Wyss JM, Cowan WM (1978) An autoradiographic study of the organization of intrahippocampal association pathways in the rat. *J Comp Neurol* 181:681–715.
- Teyler TJ, DiScenna P (1986) The hippocampal memory indexing theory. *Behav Neurosci* 100:147–154.
- Teyler TJ, Cavus I, Coussens C (1995) Synaptic plasticity in the hippocampal slice: functional consequences. *J Neurosci Methods* 59:11–17.
- Teyler TJ, Vardaris RM, Lewis D, Rawitch AB (1980) Gonadal steroids: effects on excitability of hippocampal pyramidal cells. *Science* 209:1017–1018.
- Thiels E, Barrionuevo G, Berger TW (1994) Excitatory stimulation during postsynaptic inhibition induces long-term depression in hippocampus in vivo. *J Neurophysiol* 72:3009–3016.
- Traub RD, Miles R (1991) *Neuronal networks of the hippocampus*. New York, NY: Cambridge University Press.
- Urban NN, Barrionuevo G (1996) Induction of hebbian and non-hebbian mossy fiber long-term potentiation by distinct patterns of high-frequency stimulation. *J Neurosci* 16:4293–4299.
- Weiland NG, Orikasa C, Hayashi S, McEwen BS (1997) Distribution and hormone regulation of estrogen receptor immunoreactive cells in the hippocampus of male and female rats. *J Comp Neurol* 388:603–612.
- Wong M, Moss RL (1991) Electrophysiological evidence for a rapid membrane action of the gonadal steroid, 17 beta-estradiol, on CA1 pyramidal neurons of the rat hippocampus. *Brain Res* 543:148–152.
- Wong M, Moss RL (1992) Long-term and short-term electrophysiological effects of estrogen on the synaptic properties of hippocampal CA1 neurons. *J Neurosci* 12:3217–3225.
- Woodside BL, Borroni AM, Hammonds MD, Teyler TJ (2004) NMDA receptors and voltage-dependent calcium channels mediate different aspects of acquisition and retention of a spatial memory task. *Neurobiol Learn Mem* 81:105–114.
- Woolley CS, Weiland NG, McEwen BS, Schwartzkroin PA (1997) Estradiol increases the sensitivity of hippocampal CA1 pyramidal cells to NMDA receptor-mediated synaptic input: correlation with dendritic spine density. *J Neurosci* 17:1848–1859.
- Wu TW, Wang JM, Chen S, Brinton RD (2005) 17Beta-estradiol induced Ca²⁺ influx via L-type calcium channels activates the Src/ERK/cyclic-AMP response element binding protein signal pathway and BCL-2 expression in rat hippocampal neurons: a potential initiation mechanism for estrogen-induced neuroprotection. *Neuroscience* 135:59–72.
- Xie X, Berger TW, Barrionuevo G (1992) Isolated NMDA receptor-mediated synaptic responses express both LTP and LTD. *J Neurophysiol* 67:1009–1013.
- Xie X, Barrionuevo G, Berger TW (1996) Differential expression of short-term potentiation by AMPA and NMDA receptors in dentate gyrus. *Learn Mem* 3:115–123.
- Xie X, Liaw JS, Baudry M, Berger TW (1997) Novel expression mechanism for synaptic potentiation: alignment of presynaptic release site and postsynaptic receptor. *Proc Natl Acad Sci U S A* 94:6983–6988.
- Yeckel MF, Berger TW (1998) Spatial distribution of potentiated synapses in hippocampus: dependence on cellular mechanisms and network properties. *J Neurosci* 18:438–450.
- Yoshino M, Sawada S, Yamamoto C, Kamiya H (1996) A metabotropic glutamate receptor agonist DCG-IV suppresses synaptic transmission at mossy fiber pathway of the guinea pig hippocampus. *Neurosci Lett* 207:70–72.
- Zalutsky RA, Nicoll RA (1990) Comparison of two forms of long-term potentiation in single hippocampal neurons [erratum appears in *Science*. 1991 Feb 22;251(4996):856]. *Science* 248:1619–1624.
- Zhang JQ, Cai WQ, Zhou de S, Su BY (2002) Distribution and differences of estrogen receptor beta immunoreactivity in the brain of adult male and female rats. *Brain Res* 935:73–80.
- Zhao L, Wu TW, Brinton RD (2004) Estrogen receptor subtypes alpha and beta contribute to neuroprotection and increased Bcl-2 expression in primary hippocampal neurons. *Brain Res* 1010:22–34.
- Zhao L, Chen S, Ming Wang J, Brinton RD (2005) 17beta-Estradiol induces Ca²⁺ influx, dendritic and nuclear Ca²⁺ rise and subsequent cyclic AMP response element-binding protein activation in hippocampal neurons: a potential initiation mechanism for estrogen neurotrophism. *Neuroscience* 132:299–311.